NIH Public Access
Author Manuscript
*J Mol Cell Cardiol*. Author manuscript; available in PMC 2009 December 1.

Published in final edited form as:
*J Mol Cell Cardiol*. 2008 December ; 45(6): 796–803. doi:10.1016/j.yjmcc.2008.09.124.

# PICOT is a critical regulator of cardiac hypertrophy and cardiomyocyte contractility

**Hyeseon Cha**[1], **Ji Myoung Kim**[1], **Jae Gyun Oh**[1], **Moon Hee Jeong**[1], **Chang Sik Park**[1], **Jaeho Park**[2], **Hyeon Joo Jeong**[1], **Byung Keon Park**[3], **Young-Hoon Lee**[3], **Dongtak Jeong**[2], **Dong Kwon Yang**[1], **Oliver Y. Bernecker**[4], **Do Han Kim**[1], **Roger J. Hajjar**[2], and **Woo Jin Park**[1]

[1] Global Research Laboratory and Department of Life Science, Gwangju Institute of Science and Technology, Gwangju, Korea

[2] Cardiovascular Institute, Mount Sinai School of Medicine of NYU, New York, USA

[3] Department of Oral Anatomy, School of Dentistry, Chonbuk National University, Jeonju, Korea

[4] Department of Cardiac Surgery, University of Innsbruck School of Medicine, Innsbruck, Austria

## Abstract

PICOT (PKC-interacting cousin of thioredoxin) was previously shown to inhibit the development of cardiac hypertrophy, concomitant with an increase in cardiomyocyte contractility. To explore the physiological function of PICOT in the hearts, we generated a *PICOT*-deficient mouse line by using a gene trap approach. *PICOT*$^{-/-}$ mice were embryonic lethal indicating that PICOT plays an essential role during embryogenesis, whereas *PICOT*$^{+/-}$ mice were viable with no apparent morphological defects. The PICOT protein levels were reduced by about 50% in the hearts of *PICOT*$^{+/-}$ mice. Significantly exacerbated cardiac hypertrophy was induced by pressure overload in *PICOT*$^{+/-}$ mice relative to that seen in wild type littermates. In line with this observation, calcineurin-NFAT signaling was greatly enhanced by pressure overload in the hearts of *PICOT*$^{+/-}$ mice. Cardiomyocytes from *PICOT*$^{+/-}$ mice exhibited significantly reduced contractility, which may be due in part to hypophosphorylation of phospholamban and reduced SERCA activity. These data indicate that the precise PICOT protein level significantly affects the process of cardiac hypertrophy and cardiomyocyte contractility. We suggest that PICOT plays as a critical negative regulator of cardiac hypertrophy and a positive inotropic regulator.

### Keywords

cardiac hypertrophy; PICOT; contractility; calcineurin; NFAT

## Introduction

The myocardium undergoes hypertrophic growth in response to a variety of pathological insults, including hypertension, ischemic heart disease, valvular insufficiency, and cardiomyopathy [1]. At the single cell level, cardiac hypertrophy is characterized by increased

Address correspondence to: Woo Jin Park, Department of Life Science, Gwangju Institute of Science and Technology (GIST), 1 Oryong-dong, Buk-gu, Gwangju, 500-712, Korea Phone: +82-62-970-2491; Fax: +82-62-970-2484; E-mail: wjpark@gist.ac.kr.
H.C. and J.M.K. contributed equally to this study.

**Publisher's Disclaimer:** This is a PDF file of an unedited manuscript that has been accepted for publication. As a service to our customers we are providing this early version of the manuscript. The manuscript will undergo copyediting, typesetting, and review of the resulting proof before it is published in its final citable form. Please note that during the production process errors may be discovered which could affect the content, and all legal disclaimers that apply to the journal pertain.

NIH-PA Author Manuscript
NIH-PA Author Manuscript
NIH-PA Author Manuscript

NIH-PA Author Manuscript

NIH-PA Author Manuscript

NIH-PA Author Manuscript

cell diameter and length and by the re-expression of fetal genes [2,3]. While cardiac hypertrophy is thought to be initially beneficial by maintaining and/or augmenting cardiac output, sustained hypertrophy often leads to deleterious alterations in left ventricular architecture, and is consequently a leading predictor for the development of heart failure and sudden death [4–6].

We have previously shown that PICOT (PKC interacting cousin of thioredoxin) activity constitutes a negative feedback loop for cardiac hypertrophy [7]. Expression of PICOT is up-regulated upon hypertrophic stimulation, which, in turn, abrogates the development of cardiac hypertrophy. In addition, PICOT over-expression significantly enhances ventricular function and cardiomyocyte contractility. We have also shown that PICOT negatively regulates calcineurin-NFAT signaling by disrupting the interaction between MLP (muscle LIM protein) and calcineurin [8]. With these unusual characteristics, anti-hypertrophic and positive inotropic activities in the same molecule, PICOT appears to be a potential modality for preventing cardiac hypertrophy and heart failure. However, the physiological function of PICOT in the hearts has yet to be determined.

In this study, we generated and characterized *PICOT*-deficient mice. Our results revealed that PICOT is a critical negative regulator of cardiac hypertrophy and its precise protein level significantly affects the process of cardiac hypertrophy and cardiomyocyte contractility.

## Methods

### Generation of *PICOT*-deficient mice

*PICOT*-deficient mice were generated from a mouse ES cell line with gene trap insertions that were available from large scale screening efforts (clone RRF094 from Mutant Mouse Regional Resource Center, UC Davis). In this cell line, the gene trap vector is integrated into the second intron of the *PICOT* gene. The ES cells were injected into C57BL/6 blastocysts for implantation into pseudo-pregnant female mice. The resulting chimeras were bred with C57BL/6 mice and agouti offsprings were tested for transgene transmission using PCR of tail genomic DNA (Macrogen, Seoul, Korea). The gene disruption was confirmed by genomic PCR using primer pairs (Ex2F: 5′-CAC TCC TTG TGG TTC ATT TCT GG-3′, GT-R1: 5′-CCA GGG TTT TCC CAG TCA CGA C-3′) and direct sequencing of the mutated locus. For genotyping, genomic DNA was extracted from mouse tails and subjected to PCR using primer pairs specific for the wild type sequence (In2-F: 5′-TTG TCC GTC CCT ATA AGT AAC CA-3′, In2-R: 5′-CCC GAC AAT CCA GCA GTA GC-3′) and for the mutated sequence (In2-F, and GT-R2: 5′-CGG AAG AGG CTG GAG AAG G-3′). The presence of gene trap vector was confirmed by PCR using vector-specific primers (Geo-F: 5′-ACT ATC CCG ACC GCC TTA-3′, Geo-R: 5′-TAG CGG CTG ATG TTG AAC TG-3′). Animal handling and experimentation were performed according to the regulations of Gwangju Institute of Science and Technology.

### Transverse aortic banding

Male mice of 8–10 weeks of age (25–32 g) were used for the study. The animals were anesthetized with 0.5ml–0.7ml of 1X Avertin solution (mixture of 2-2-2 tribromoethanol and tert-amyl alcohol) by intraperitoneal injection. Mice were ventilated with a tidal volume of 0.1 ml and a respiratory rate of 120 breaths per minute (Harvard Apparatus). A 2- to 3-mm longitudinal cut was made in the proximal portion of the sternum which allowed visualization of the aortic arch. The transverse aortic arch was ligated between the innominate and left common carotid arteries with an overlaying 27-gauge needle, and then the needle was immediately removed leaving a discrete region of constriction. One week post-operation mortality was less than 10%.

NIH-PA Author Manuscript

NIH-PA Author Manuscript

NIH-PA Author Manuscript

### Histological analysis of hearts

Hearts were arrested at end diastole and the left ventricle was freed from the right ventricle and weighed. Paraffin or glycol methacrylate-embedded (Technovit 8100) hearts were cut into 4 μm and 1.5 μm slices, respectively. The sections were stained with hematoxylin-eosin solution. To measure the surface area of cardiomyocytes, suitable cross sections with nearly circular capillary profiles and nuclei were selected, observed under an Axiophot microscope (Carl Zeiss), and analyzed with AnalysisSIS3.2 software (Soft-Imaging System).

### Quantitative RT-PCR

Total RNA was isolated with TRI reagent (Sigma). Reverse-transcription was performed using ImProm II reverse-transcriptase (Promega) with oligo-dT priming. PCR was performed using an ABI PRISM Sequence Dectector System 7500 (Applied Biosystems) with SYBR Green (Takara) as fluorescent and ROX (Takara) as reference dyes. PCR primers used were: ANF, 5′-CTG CTT CGG GGG TAG GAT TG-3′ and 5′-TGA CAC ACC ACA AGG GC-3′; SKA, 5′-TCA GGC GGT GCT GTC TCT CT-3′ and 5′-TCC CCA GAA TCC AAC ACG AT-3′; MCIP1, 5′-TCC AGC TTG GGC TTG ACT GAG-3′ and 5′-ACT GGA AGG TGG TGT CCT TGT C-3′.

### Calcineurin phosphatase activity assay

The Biomol green calcineurin assay kit (cat. # AK-816, Biomol) was used to determine the calcineurin phosphatase activity according to the manufacturer's instruction. The RII phosphopeptide was used as a specific substrate for calcineurin.

### Isolation of adult mouse ventricular myocytes

Ventricular myocytes were isolated from mouse hearts using the method described by Ren [9] with minor modifications. Male mice of 8–12 weeks of age (25–32 g) were used for the study. In brief, after heparin (50 units) injection, animals were sacrificed by cervical dislocation. The heart was quickly removed from the chest and the aorta was retrogradely perfused at 37°C for 3 min with calcium-free Tyrode buffer (137 mM NaCl, 5.4 mM KCl, 1 mM $MgCl_2$, 10 mM glucose, 10 mM HEPES, 10mM 2, 3-butanedione monoxime (BDM; Sigma), and 5mM taurine (Sigma) (pH 7.4)) gassed with 95% $O_2$/5% $CO_2$. The enzymatic digestion was initiated by adding collagenase type B (0.35 U/ml; Roche) and hyaluronidase (0.1 mg/ml; Sigma) to the perfusion solution. When the heart became swollen after 10 min of digestion, the left ventricle was quickly removed, cut into several chunks, and further digested in a shaker (60–70 rpm) for 10 min at 37°C in the same enzyme solution. The supernatant containing the dispersed myocytes was filtered through a cell strainer (100μm, BD Falcon) and gently centrifuged at 500 rpm for 1 min. Extracellular $Ca^{2+}$ was incrementally added back to 1.25 mM over a span of 30min to avoid $Ca^{2+}$ paradox. This procedure usually yielded more than 50% viable rod- shaped ventricular myocytes with clear sarcomere striations. Myocytes with obvious sarcolemmal blebs or spontaneous contraction were not used.

### Cell contractility and intracellular $Ca^{2+}$ transient measurement

The mechanical properties of ventricular myocytes were assessed using a video-based edge detection system (IonOptix) as previously described [10]. In brief, laminin-coated coverslips with cells attached were placed in a chamber mounted on the stage of an inverted microscope (Nikon Eclipse TE-100F) and superfused (about 1 ml/min at 25°C) with Tyrode buffer (137 mM NaCl, 5.4 mM KCl, 1 mM $CaCl_2$, 1 mM $MgCl_2$, 10 mM glucose, and10 mM HEPES (pH 7.4)). The cells were field stimulated at a frequency of 1 Hz (30 V) using a STIM-AT stimulator/thermostat placed on HLD-CS culture chamber/stim holder (Cell MicroControls). The myocyte under study was displayed on a computer monitor using an IonOptix MyoCam camera, which rapidly scanned the image area every 8.3 ms, such that the amplitude and velocity of shortening

NIH-PA Author Manuscript

NIH-PA Author Manuscript

NIH-PA Author Manuscript

or relengthening were recorded with good fidelity. Changes in cell length during shortening and relengthening were captured and analyzed using soft edge software (IonOptix). The cardiomyocytes were loaded with 0.5 μM fura2-AM (Molecular Probes), a $Ca^{2+}$-sensitive indicator, for 15 min at 25°C. Fluorescence measurements were recorded using IonOptix simultaneously with contractility measurements. Cardiomyocytes were placed on an inverted microscope and were exposed to light emitted by a 75 W halogen lamp through either a 360 or 380 nm filter while being stimulated to contract at 0.5 Hz. Fluorescence emissions were detected between 480 and 520 nm by a photomultiplier tube after initial illumination at 360 nm for 0.5 s and then at 380 nm for the duration of the recording protocol. The 360 nm excitation scan was repeated at the end of the protocol and qualitative changes in the intracellular $Ca^{2+}$ concentration were inferred from the ratio of the fura fluorescence intensity (FFI) at both wavelengths.

### $Ca^{2+}$ uptake assay

Oxalate-supported $Ca^{2+}$ uptake measurements in cardiac homogenates were performed as described [11] with a minor modification. Briefly, frozen cardiac powder was homogenized in 50 mM potassium phosphate (pH 7.0), 10 mM NaF, 1 mM EDTA, 0.3 M sucrose, 0.3 mM PMSF, and 0.5 mM DTT. $Ca^{2+}$ uptake in tissue homogenates (0.1 mg/ml) was measured by the Millipore filtration technique. The reaction mixture contained 20 mM MOPS (pH 7.0), 100 mM KCl, 10 mM $NaN_3$, 1 μM ruthenium red, 5 mM K-Oxalate, 0.2 mM $CaCl_2$. Homogenates were incubated at 37°C for 4 minutes in the above buffer, and the reaction was initiated by the addition of Mg-ATP (final concentration, 5 mM). The rates of $Ca^{2+}$ uptake were calculated by least squares linear regression analysis of uptake values at 30, 60, 90 and 120 seconds. The results were analyzed using SigmaPlot 10 software.

### Western blot analysis

Cardiac whole homogenate samples (50μg) in SDS sample buffer were run on an SDS-PAGE gel, and proteins in the gel were transferred to PVDF membrane (Bio-Rad). The membrane was blocked with 5% skim milk and incubated overnight with an antibody directed against RyR (Affinity Bioreagents), FKBP12 (Santa Cruz), DHPR (Affinity Bioreagents), phospholamban (Affinity Bioreagents), phospho-PLB ($Thr^{17}$, Badrilla), phospho-PLB ($Ser^{16}$, Cell Signaling), Troponin I (Cell Signaling), phospho-Troponin I ($Ser^{23,24}$, Cell Signaling), SERCA (Affinity Bioreagents), $Na^{2+}$-$Ca^{2+}$ exchanger (Affinity Bioreagent), triadin (Santa Cruz), α-tubulin (Santa Cruz), GAPDH (Sigma), or PICOT. The membrane was then incubated with a secondary antibody conjugated to horseradish peroxidase (Jackson ImmunoResearch) and developed using Western Lighting™ Chemiluminescence Reagent (PerkinElmer).

### Statistics

All data are reported as mean ± SD. Statistical significance was analyzed by Student's unpaired t test or one-way ANOVA with a Bonferroni post-test analysis (Statview V5.0, SAS). $P<0.05$ was considered statistically significant.

## Results

### Disruption of the *PICOT* gene

One *PICOT*-deficient line was generated by using the gene trap approach. In this line, the gene trap disrupted the *PICOT* gene within the second intron. To confirm this gene disruption, genomic DNA containing the gene trap insertion was amplified using a forward primer specific to exon 2 (Ex2-F) and a reverse primer specific to the gene trap vector (GT-R1). Directed nucleotide sequencing of the amplified PCR product revealed that the gene trap insertion had

NIH-PA Author Manuscript

NIH-PA Author Manuscript

NIH-PA Author Manuscript

occurred 1,672 bp downstream of exon 2 (Figure 1A). Genotyping was conducted by performing genomic PCR. A pair of forward (In2-F) and reverse primers (In2-R) specific to PICOT intron 2 were designed to generate a wild type PCR product of 500 bp. A reverse primer (GT-R2) specific to the gene trap vector was used together with the forward primer In2-F to generate a mutant PCR product of 620 bp. The presence of the gene trap vector was also confirmed by PCR using a primer pair (Geo-F and Geo-R) specific to the trap vector, which resulted in a PCR product of 171 bp (Figure 1B).

Genotyping of 132 live-born mice from intercrosses between *PICOT*$^{+/-}$ mice identified 43 *PICOT*$^{+/+}$ and 89 *PICOT*$^{+/-}$ mice but no *PICOT*$^{-/-}$ mice (Figure 1C). The ratio of *PICOT*$^{+/+}$ to *PICOT*$^{+/-}$ mice (43:89) fits the expected ratio of 1:2, which is suggestive of a purely recessive lethality in the homozygote. *PICOT*$^{+/-}$ mice were fertile and showed no abnormalities in growth and development. To identify the stages of embryogenesis at which the lethality occurs in *PICOT*$^{-/-}$ embryos, embryos at different developmental stages were examined. At E9.5 and E12.5, the embryos showed genotypic ratios not significantly different from the normal Mendelian ratio. At E14.5, however, no *PICOT*$^{-/-}$ embryos were identified (Figure 1C). These data suggest that the *PICOT*$^{-/-}$ embryos died sometime between E12.5 and E14.5. Histological analysis of E12.5 *PICOT*$^{-/-}$ embryo sections stained with hematoxylin and eosin revealed no defects in organogenesis (data not shown). The apparent defects of E12.5 *PICOT*$^{-/-}$ embryos were a smaller body size and hemorrhage in the head. These data indicate that *PICOT* plays an essential role during embryogenesis. Due to the embryonic lethality of *PICOT*$^{-/-}$, all the following experiments were conducted with PICOT$^{+/-}$ mice.

## Exacerbated response of *PICOT*$^{+/-}$ mice to pressure-overload

PICOT protein levels measured by Western blot analysis were approximately 50% lower in the hearts of 8 week old *PICOT*$^{+/-}$ mice compared to the age-matched wild type littermates (Figure 2A). We examined the hypertrophic response of *PICOT*$^{+/-}$ mice with a pressure-overload model of cardiac hypertrophy. Transverse aortic banding (TAB) resulted in an approximately 38% increase in the heart weight to body weight ratio in wild type mice over 7 days. This hypertrophic growth was exacerbated significantly ($p<0.01$ vs. *PICOT*$^{+/+}$ TAB) in *PICOT*$^{+/-}$ mice with an approximately 65% increase in the heart weight to body weight ratio (Figure 2B). Furthermore, microscopic analysis of histological sections revealed that the increase in the ventricular cross-sectional area was exacerbated significantly ($p<0.01$ vs. *PICOT*$^{+/+}$ TAB) in *PICOT*$^{+/-}$ mice (a 154% increase in TAB vs. sham) compared with wild type mice (a 60% increase in TAB vs. sham) (Figure 2C). Quantitative PCR analysis showed that the induction of hypertrophic markers, ANF and SKA (skeletal actin), by pressure-overload was greatly enhanced in *PICOT*$^{+/-}$ mice (479% and 210% increases of ANF and SKA, respectively, in TAB vs. sham) compared with wild type mice (281 % and 43% increases of ANF and SKA, respectively, in TAB vs. sham) (Figure 2D). These results indicate that a 50% reduction in the PICOT protein level results in dramatic exacerbation of cardiac hypertrophy, implying that PICOT is an essential anti-hypertrophic molecule. These results are also conversely consistent with our previous finding that overexpression of PICOT in the heart abrogated the development of cardiac hypertrophy [7]. We have previously shown that PICOT inhibits cardiac hypertrophy by disrupting calcineurin-NFAT signaling pathway [8]. Therefore, we examined whether the exacerbated cardiac hypertrophy in *PICOT*$^{+/-}$ mice is associated with enhanced calcineurin-NFAT signaling. Calcineurin phosphatase activity was greatly increased in *PICOT*$^{+/-}$ mice (a 66% increase in TAB vs. sham) compared with wild type mice (a 42% increase in TAB vs. sham) (Figure 3A). Quantitative PCR analysis also showed that the induction of a known transcriptional target of NFAT, MCIP, by pressure overload was greatly increased in *PICOT*$^{+/-}$ mice (16-fold increase in TAB vs. sham) compared with wild type littermates (10-fold increase in TAB vs. sham) (Figure 3B).

NIH-PA Author Manuscript

NIH-PA Author Manuscript

NIH-PA Author Manuscript

### Reduced cardiomyocyte contractility of *PICOT*$^{+/-}$ mice

We have previously shown that ventricular function and cardiomyocyte contractility are significantly enhanced in transgenic mice overexpressing PICOT in the heart [7]. Therefore, we examined whether the ventricular and contractile functions were affected by the reduced PICOT protein level. Adult cardiomyocytes were isolated and their contractile properties were determined using a dual-excitation spectrofluorometer equipped with video-edge detection system. *PICOT*$^{+/-}$ cardiomyocytes showed a 23% decrease in cell shortening, a 29% decrease in maximal rate of contraction (−dL/dt), and a 36% decrease in maximal rate of relaxation (+dL/dt) in comparison with *PICOT*$^{+/+}$ littermates (Figure 4A). Analyses of intracellular $Ca^{2+}$ handling revealed that $Ca^{2+}$ transient decay, τ, but not the baseline $Ca^{2+}$ content and the $Ca^{2+}$ transient amplitude, increased by approximately 29% in *PICOT*$^{+/-}$ cardiomyocytes (Figure 4B). Consistent with the increased τ, SR $Ca^{2+}$ reuptake activity was reduced by approximately 39% in *PICOT*$^{+/-}$ cardiomyocytes (Figure 4C). Cell shortening was plotted against cytosolic $Ca^{2+}$ content during steady-state contraction. A downward shift of the loop in *PICOT*$^{+/-}$ cardiomyocytes indicated the reduced cell shortening at any given $Ca^{2+}$ concentration, implying a decrease in $Ca^{2+}$ sensitivity of the *PICOT*$^{+/-}$ filaments (Figure 4D). These data are conversely consistent with our previous findings obtained with PICOT transgenic mice. We further investigated the effect of pressure overload on the cardiomyocyte contractility. While the contractile parameters were slightly reduced by TAB in *PICOT*$^{+/+}$ cardiomyocytes, they were significantly restored by TAB in *PICOT*$^{+/-}$ cardiomyocytes albeit still significantly lower that those of wild type littermates (Figure 4E). The molecular mechanism underlying the restoration of contractility by TAB in *PICOT*$^{+/-}$ cardiomyocytes remains to be explored.

To address whether the reduction in contractility in *PICOT*$^{+/-}$ cardiomyocytes is associated with changes in the expression level of excitation-coupling proteins, major $Ca^{2+}$-handling proteins were probed by immunoblotting. Among the tested proteins, only the phosphorylation of phospholamban (PLB) at threonine 17 was significantly reduced in *PICOT*$^{+/-}$ cardiomyocytes (Figure 5). PLB is known to be phosphorylated at threonine 17 by $Ca^{2+}$-calmodulin-dependent protein kinase (CaMKII) [12,13]. Targeted inhibition of CaMKII by a specific inhibitory peptide resulted in a decreased PLB phosphorylation at threonine 17 and consequently mild cardiac dysfunction and reduced cardiomyocyte contractility [14,15]. Therefore, the decreased PLB phosphorylation at threonine 17 in *PICOT*$^{+/-}$ mice appears to contribute to the reduced cardiomyocyte contractility.

## Discussion

In our previous study, we suggested that PICOT constitutes a feedback inhibitory mechanism of cardiac hypertrophy [7]. PICOT was shown to be induced during the development of cardiac hypertrophy. Adenovirus-mediated PICOT overexpression completely blocked the hypertrophic response of neonatal cardiomyocytes to endothelin-1 and phenylephrine. In addition, PICOT overexpression in the heart using the transgenic approach also blocked cardiac hypertrophy induced by pressure overload.

In this study, we generated *PICOT* knockout mice to explore the physiological role of PICOT in the hearts. Embryonic lethality of *PICOT* homozygote mice suggested that PICOT plays an essential role during embryogenesis. Detailed histological analysis is underway to elucidate anatomical defects in these mice. To our surprise, we observed that the hypertrophic response to pressure overload is greatly enhanced in *PICOT*$^{+/-}$ mice which contain about half of the normal PICOT protein level. These data suggest that PICOT is a critical negative regulator and that its precise protein level significantly affects the process of cardiac hypertrophy. Most of the phenotypic differences between *PICOT*$^{+/-}$ mice and its littermates were distinct only during the early phase of hypertrophic responses (1–2 weeks after TAB), probably because the PICOT

NIH-PA Author Manuscript

NIH-PA Author Manuscript

NIH-PA Author Manuscript

protein level in *PICOT*$^{+/-}$ mice under pressure overload gradually caught up with that of wild type littermates. There was no significant difference in the PICOT protein levels between the two groups at 4 weeks after TAB (data not shown). Therefore, we could not observe long-term effects of PICOT deletions on the development of cardiac hypertrophy and heart failure in this study. About 10–20% of *PICOT*$^{+/-}$ mice showed severe wall dilation and died within 2 weeks of TAB (Supplementary Figure 1), suggesting that lack of PICOT is detrimental. Mortality of wild type littermates under the same condition was about 5% and none of the dead mice showed significant heart failure phenotypes.

Muscle LIM protein (MLP) is essential for cardiac cytoarchitectural organization, and deficiency in this protein leads to defects in the mechanical stretch response and eventually to dilated cardiomyopathy [16]. Recently, MLP was found to be essential for calcineurin anchorage to the Z-disc and appropriate calcineurin-NFAT signaling [17]. Calcineurin, the $Ca^{2+}$/calmodulin-dependent phosphatase, plays a pivotal role in cardiac hypertrophy by promoting dephosphorylation and nuclear translocation of NFAT [18,19]. We found that PICOT directly binds to MLP which in turn inhibits MLP-calcineurin binding, resulting in abrogation of calcineurin-NFAT signaling. Therefore, it appears that PICOT inhibits cardiac hypertrophy largely by abrogating calcineurin-NFAT signaling [8]. In this study, we found that calcineurin-NFAT signaling is greatly induced by pressure overload, indicating that PICOT indeed plays a critical role in the regulation of calcineurin-NFAT signaling.

We have previously shown that PICOT overexpression dramatically increases ventricular function and cardiomyocyte contractility [7]. In the converse situation described here, a 50% reduction in the PICOT protein level resulted in reduced contractility of isolated cardiomyocytes. The reduced contractility in *PICOT*$^{+/-}$ cardiomyocytes was slightly restored under pressure overload, but was still significantly lower than that of wild type littermates. We propose that PICOT may affect cardiomyocyte contractility in two ways. First, PICOT increases calcium sensitivity of the contractile filaments (Figure 4D) [7] probably via altering the phosophorylation status of some contractile proteins. For example, troponin I was found to be hyperphosphorylated in PICOT transgenic hearts (data not shown). Second, PICOT increases the SERCA activity (Figure 4C) probably through regulating the PLB activity. Interestingly, PLB phosphorylation at threonine 17 but not at serine 16 was reduced in *PICOT*$^{+/-}$ cardiomyocytes (Figure 5). It is known that PLB can be phosphorylated at serine 16 by cAMP-dependent protein kinase (PKA) and at threonine 17 by CaMKII [12,13]. Inhibition of CaMKII by a specific peptide resulted in reduction of PLB phosphorylation at threonine 17, and cardiac dysfunction and reduced contractility [14,15]. Therefore, it is possible that the observed reduction of PLB phosphorylation at threonine 17 is a direct cause of the reduced SERCA activity and cardiomyocyte contractility. However, this is contradictory to the finding that no reduction of contractile parameters was observed in transgenic mice expressing the T17A mutant PLB in the hearts [20]. Further studies are warranted to elucidate the mechanism underlying the PICOT-mediated regulation of cardiac function and cardiomyocyte contractility.

Our data confirm the notion that PICOT plays as a critical negative regulator of cardiac hypertrophy and a positive inotropic regulator.

## Supplementary Material

Refer to Web version on PubMed Central for supplementary material.

NIH-PA Author Manuscript

NIH-PA Author Manuscript

NIH-PA Author Manuscript

## Acknowledgments

During this work, W.J.P. was supported by the Global Research Laboratory Program (M6-0605-00-0001) of the Korean Ministry of Science and Technology. R.J.H. and W.J.P. were supported by a NIH grant HL-080498-01. D.H.K. was supported by a Korean Systems Biology Research grant (M10503010001-07N0301-00110).

## References

1. Heineke J, Molkentin JD. Regulation of cardiac hypertrophy by intracellular signalling pathways. Nature reviews 2006 Aug;7(8):589–600.
2. Zimmer HG, Gerdes AM, Lortet S, Mall G. Changes in heart function and cardiac cell size in rats with chronic myocardial infarction. Journal of molecular and cellular cardiology 1990 Nov;22(11):1231–43. [PubMed: 2149393]
3. Rockman HA, Ross RS, Harris AN, Knowlton KU, Steinhelper ME, Field LJ, et al. Segregation of atrial-specific and inducible expression of an atrial natriuretic factor transgene in an in vivo murine model of cardiac hypertrophy. Proceedings of the National Academy of Sciences of the United States of America 1991 Sep 15;88(18):8277–81. [PubMed: 1832775]
4. Lips DJ, deWindt LJ, van Kraaij DJ, Doevendans PA. Molecular determinants of myocardial hypertrophy and failure: alternative pathways for beneficial and maladaptive hypertrophy. European heart journal 2003 May;24(10):883–96. [PubMed: 12714020]
5. Berenji K, Drazner MH, Rothermel BA, Hill JA. Does load-induced ventricular hypertrophy progress to systolic heart failure? American journal of physiology 2005 Jul;289(1):H8–H16. [PubMed: 15961379]
6. Haider AW, Larson MG, Benjamin EJ, Levy D. Increased left ventricular mass and hypertrophy are associated with increased risk for sudden death. Journal of the American College of Cardiology 1998 Nov;32(5):1454–9. [PubMed: 9809962]
7. Jeong D, Cha H, Kim E, Kang M, Yang DK, Kim JM, et al. PICOT inhibits cardiac hypertrophy and enhances ventricular function and cardiomyocyte contractility. Circulation research 2006 Aug 4;99(3):307–14. [PubMed: 16809552]
8. Jeong D, Kim JM, Cha H, Oh JG, Park J, Yun SH, et al. PICOT attenuates cardiac hypertrophy by disrupting calcineurin-NFAT signaling. Circulation research 2008 Mar 28;102(6):711–9. [PubMed: 18258855]
9. Ren J, Wold LE. Measurement of Cardiac Mechanical Function in Isolated Ventricular Myocytes from Rats and Mice by Computerized Video-Based Imaging. Biological procedures online 2001 Dec 11;3:43–53. [PubMed: 12734580]
10. Zhou YY, Wang SQ, Zhu WZ, Chruscinski A, Kobilka BK, Ziman B, et al. Culture and adenoviral infection of adult mouse cardiac myocytes: methods for cellular genetic physiology. American journal of physiology 2000 Jul;279(1):H429–36. [PubMed: 10899083]
11. Luo W, Grupp IL, Harrer J, Ponniah S, Grupp G, Duffy JJ, et al. Targeted ablation of the phospholamban gene is associated with markedly enhanced myocardial contractility and loss of beta-agonist stimulation. Circulation research 1994 Sep;75(3):401–9. [PubMed: 8062415]
12. Simmerman HK, Collins JH, Theibert JL, Wegener AD, Jones LR. Sequence analysis of phospholamban. Identification of phosphorylation sites and two major structural domains. The Journal of biological chemistry 1986 Oct 5;261(28):13333–41. [PubMed: 3759968]
13. Koss KL, Kranias EG. Phospholamban: a prominent regulator of myocardial contractility. Circulation research 1996 Dec;79(6):1059–63. [PubMed: 8943944]
14. Ji Y, Li B, Reed TD, Lorenz JN, Kaetzel MA, Dedman JR. Targeted inhibition of Ca2+/calmodulin-dependent protein kinase II in cardiac longitudinal sarcoplasmic reticulum results in decreased phospholamban phosphorylation at threonine 17. The Journal of biological chemistry 2003 Jul 4;278(27):25063–71. [PubMed: 12692124]
15. Ji Y, Zhao W, Li B, Desantiago J, Picht E, Kaetzel MA, et al. Targeted inhibition of sarcoplasmic reticulum CaMKII activity results in alterations of Ca2+ homeostasis and cardiac contractility. American journal of physiology 2006 Feb;290(2):H599–606. [PubMed: 16143658]

NIH-PA Author Manuscript

NIH-PA Author Manuscript

NIH-PA Author Manuscript

16. Arber S, Hunter JJ, Ross J Jr, Hongo M, Sansig G, Borg J, et al. MLP-deficient mice exhibit a disruption of cardiac cytoarchitectural organization, dilated cardiomyopathy, and heart failure. Cell 1997 Feb 7;88(3):393–403. [PubMed: 9039266]

17. Heineke J, Ruetten H, Willenbockel C, Gross SC, Naguib M, Schaefer A, et al. Attenuation of cardiac remodeling after myocardial infarction by muscle LIM protein-calcineurin signaling at the sarcomeric Z-disc. Proceedings of the National Academy of Sciences of the United States of America 2005 Feb 1;102(5):1655–60. [PubMed: 15665106]

18. Shaw KT, Ho AM, Raghavan A, Kim J, Jain J, Park J, et al. Immunosuppressive drugs prevent a rapid dephosphorylation of transcription factor NFAT1 in stimulated immune cells. Proceedings of the National Academy of Sciences of the United States of America 1995 Nov 21;92(24):11205–9. [PubMed: 7479966]

19. Loh C, Shaw KT, Carew J, Viola JP, Luo C, Perrino BA, et al. Calcineurin binds the transcription factor NFAT1 and reversibly regulates its activity. The Journal of biological chemistry 1996 May 3;271(18):10884–91. [PubMed: 8631904]

20. Chu G, Lester JW, Young KB, Luo W, Zhai J, Kranias EG. A single site (Ser16) phosphorylation in phospholamban is sufficient in mediating its maximal cardiac responses to beta -agonists. The Journal of biological chemistry 2000 Dec 8;275(49):38938–43. [PubMed: 10988285]

NIH-PA Author Manuscript

NIH-PA Author Manuscript

NIH-PA Author Manuscript

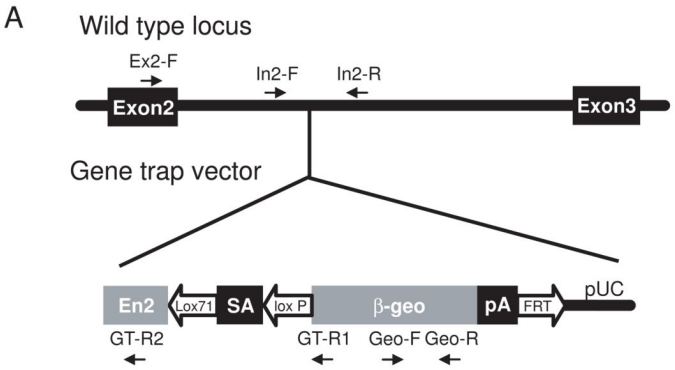


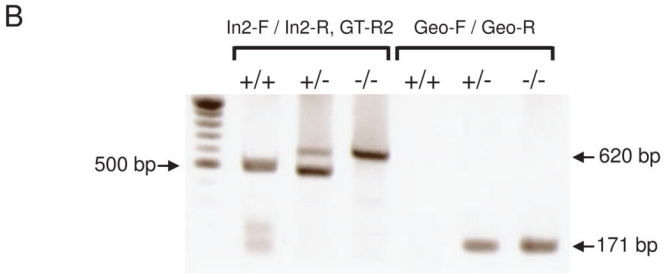


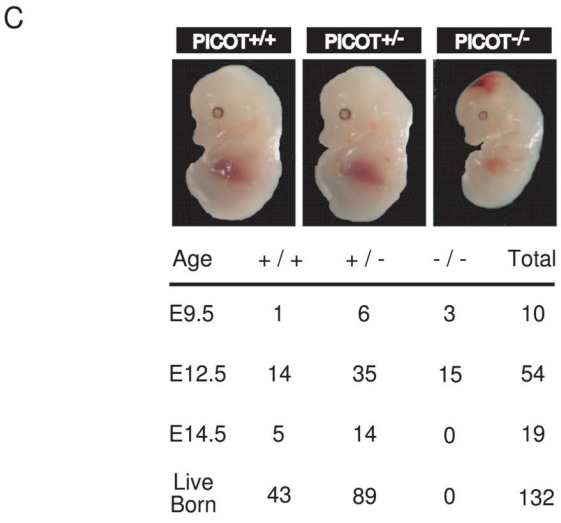


| Age | + / + | + / - | - / - | Total |
|---|---|---|---|---|
| E9.5 | 1 | 6 | 3 | 10 |
| E12.5 | 14 | 35 | 15 | 54 |
| E14.5 | 5 | 14 | 0 | 19 |
| Live Born | 43 | 89 | 0 | 132 |

**Figure 1. Targeted disruption of the *PICOT* gene**

(A) Embryonic stem cell line RRF094 contains the gene trap vector pGT0 inserted within the second intron of PICOT. The PICOT locus and pGT0 insertion are shown. The vector pGT0 contains a part of the mouse *engrailed 2* intron 1 (En2), a splice acceptor of mouse En2 exon 2 (SA), a β-galactosidase/neomycin resistance fusion gene (β-geo), and a SV40 polyadenylation sequence (pA). Arrows indicate PCR primer binding sites for genomic PCR and genotyping. (B) Representative genotypic analysis of littermates harboring the WT (+) or deleted allele (−) of the *PICOT* gene from a $PICOT^{+/-}$ intercrosses. Genotyping was performed by PCR using primers In2-F and In2-R for the wild-type (500 bp), and In2-F and GT-R2 for the deleted allele (620 bp). The presence of gene trap vector was also confirmed by PCR using

primer pairs Geo-F and Geo-R (171 bp). (C) Photographs of littermates (E12.5) from *PICOT*$^{+/-}$ intercrosses are shown. The genotype of the littermates was analyzed by PCR.

NIH-PA Author Manuscript
NIH-PA Author Manuscript
NIH-PA Author Manuscript

NIH-PA Author Manuscript
NIH-PA Author Manuscript
NIH-PA Author Manuscript



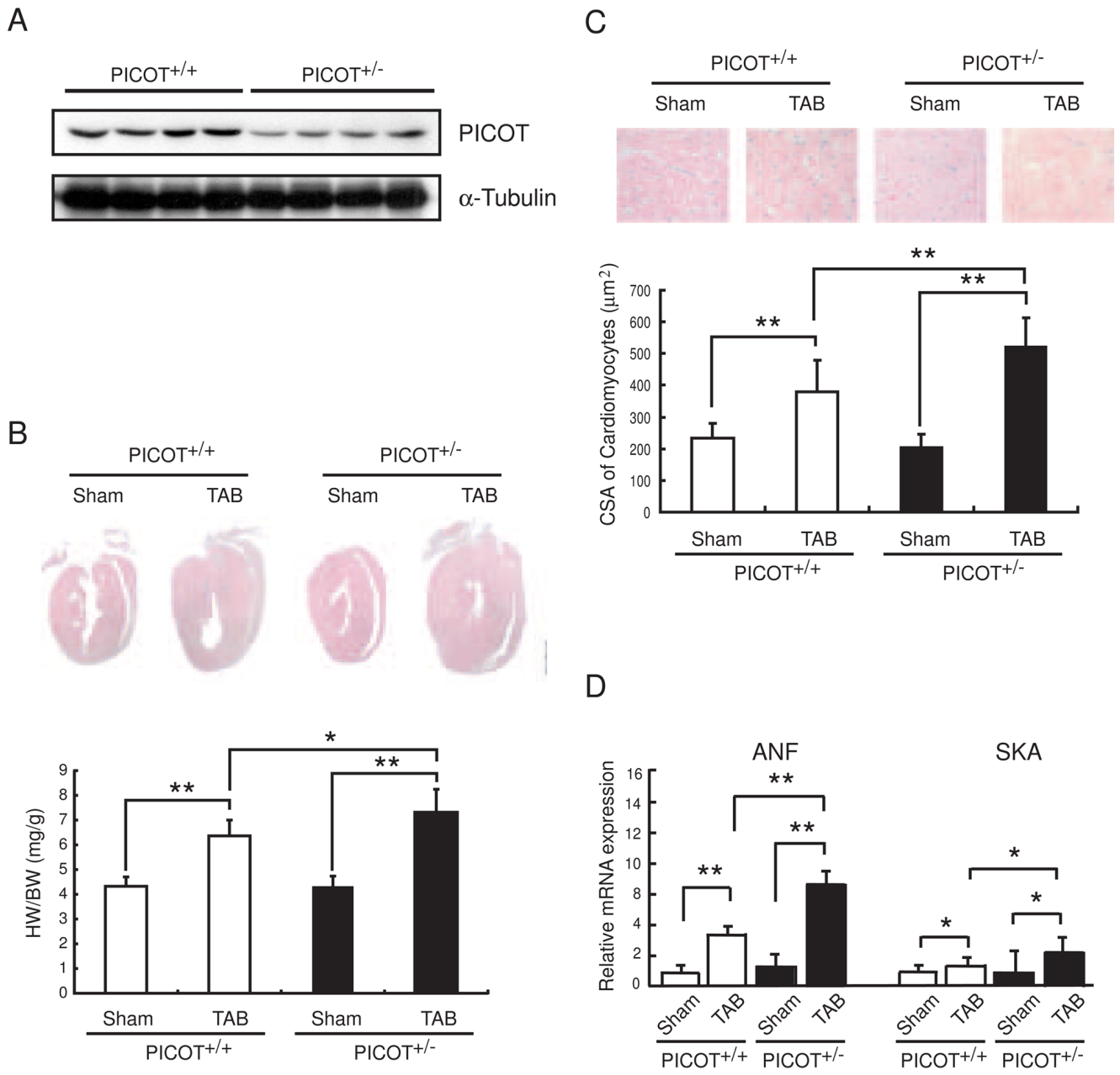


**Figure 2. Enhanced hypertrophy in *PICOT*$^{+/-}$ mice**

(A) Adult heart lysates from *PICOT*$^{+/+}$ and *PICOT*$^{+/-}$ littermates were separated by SDS-PAGE and subjected to Western blot analysis with anti-PICOT antibody. (B) Representative longitudinal sections of *PICOT*$^{+/+}$ and *PICOT*$^{+/-}$ hearts, sham operated (Sham) or transverse aortic banded for one week (TAB) are shown. The heart weight (HW) to body weight (BW) ratio is shown. n=6 per group. (C) Higher magnification photographs of the heart sections are also shown. Cell surface area (CSA) of individual cardiomyocyte was measured using the AnalSIS image analysis program. n=3 per group; about 100 cells were analyzed from each heart. (D) Expression levels of hypertrophic marker genes, ANF and SKA, were determined by quantitative RT-PCR. All the data are represented as mean ± SD. *P<0.05, **P<0.01.

NIH-PA Author Manuscript

NIH-PA Author Manuscript

NIH-PA Author Manuscript

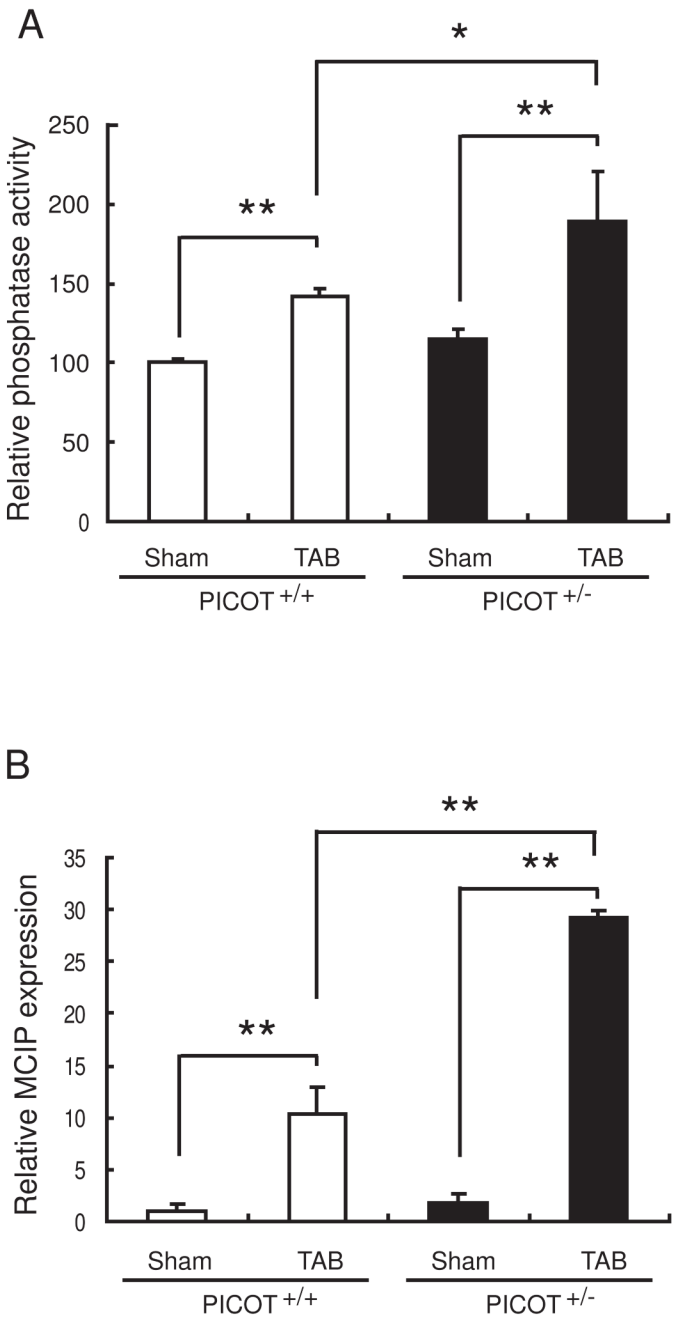


**Figure 3.**

Enhanced calcineurin-NFAT signaling in *PICOT*$^{+/-}$ mice. (A) Calcineurin phosphatase activity was determined. (B) Expression level of a transcriptional target of NFAT, MCIP, was determined by quantitative RT-PCR. All the data are represented as mean ± SD. *P<0.05, **P<0.01.

NIH-PA Author Manuscript
NIH-PA Author Manuscript
NIH-PA Author Manuscript



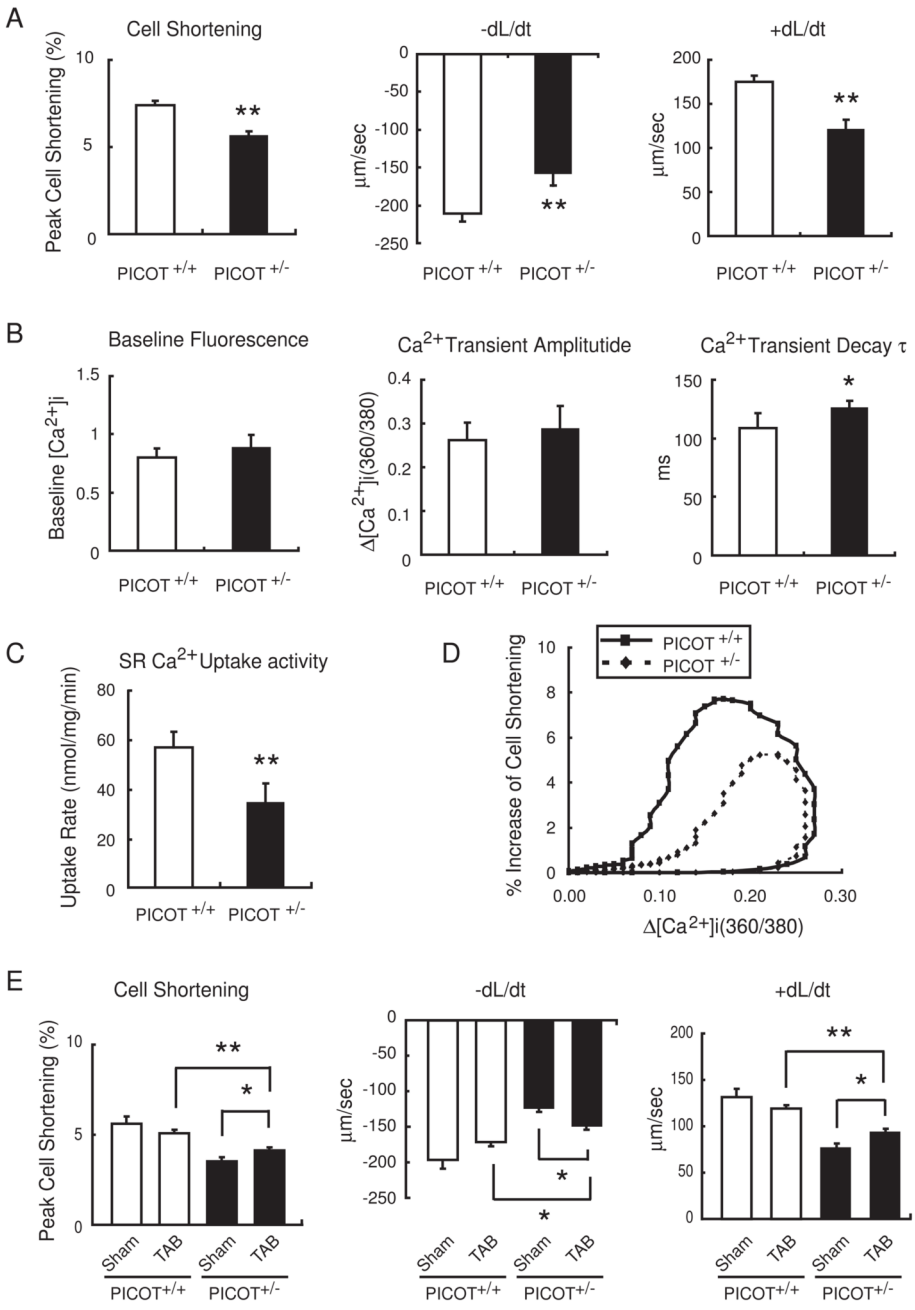


**Figure 4. Cardiomyocyte contractility and $Ca^{2+}$ transient in *PICOT*$^{+/-}$ mice**

(A) Adult cardiomyocytes were isolated from *PICOT*$^{+/+}$ and *PICOT*$^{+/-}$ littermates and their contractile parameters were determined. Peak cell shortening, percentage of shortened cell length; −dL/dt, maximal velocities of cell shortening; +dL/dt, maximal velocities of cell relengthening. (B) Average parameters of $Ca^{2+}$ transient properties were determined using fura2/acetoxymethyl ester. (C) SR $Ca^{2+}$ uptake rates were measured in the presence of 0.2 mM $CaCl_2$. (D) A plot of hysteresis loop of cell shortening against cytosolic $Ca^{2+}$ content is shown. (E) Adult cardiomyocytes were isolated from *PICOT*$^{+/+}$ and *PICOT*$^{+/-}$ littermates which were sham operated (Sham) or transverse aortic banded (TAB) for 1 week and their contractile parameters were determined. Approximately 140 cells were chosen for the contractility and

NIH-PA Author Manuscript

NIH-PA Author Manuscript

NIH-PA Author Manuscript

$Ca^{2+}$ transient measurements from seven individual hearts per group. All the data are represented as mean ± SD. For panels A–C, *P<0.05 vs *PICOT*$^{+/+}$ and **P<0.01 vs *PICOT*$^{+/+}$. For panel E, *P<0.05 and **P<0.01.

NIH-PA Author Manuscript
NIH-PA Author Manuscript
NIH-PA Author Manuscript



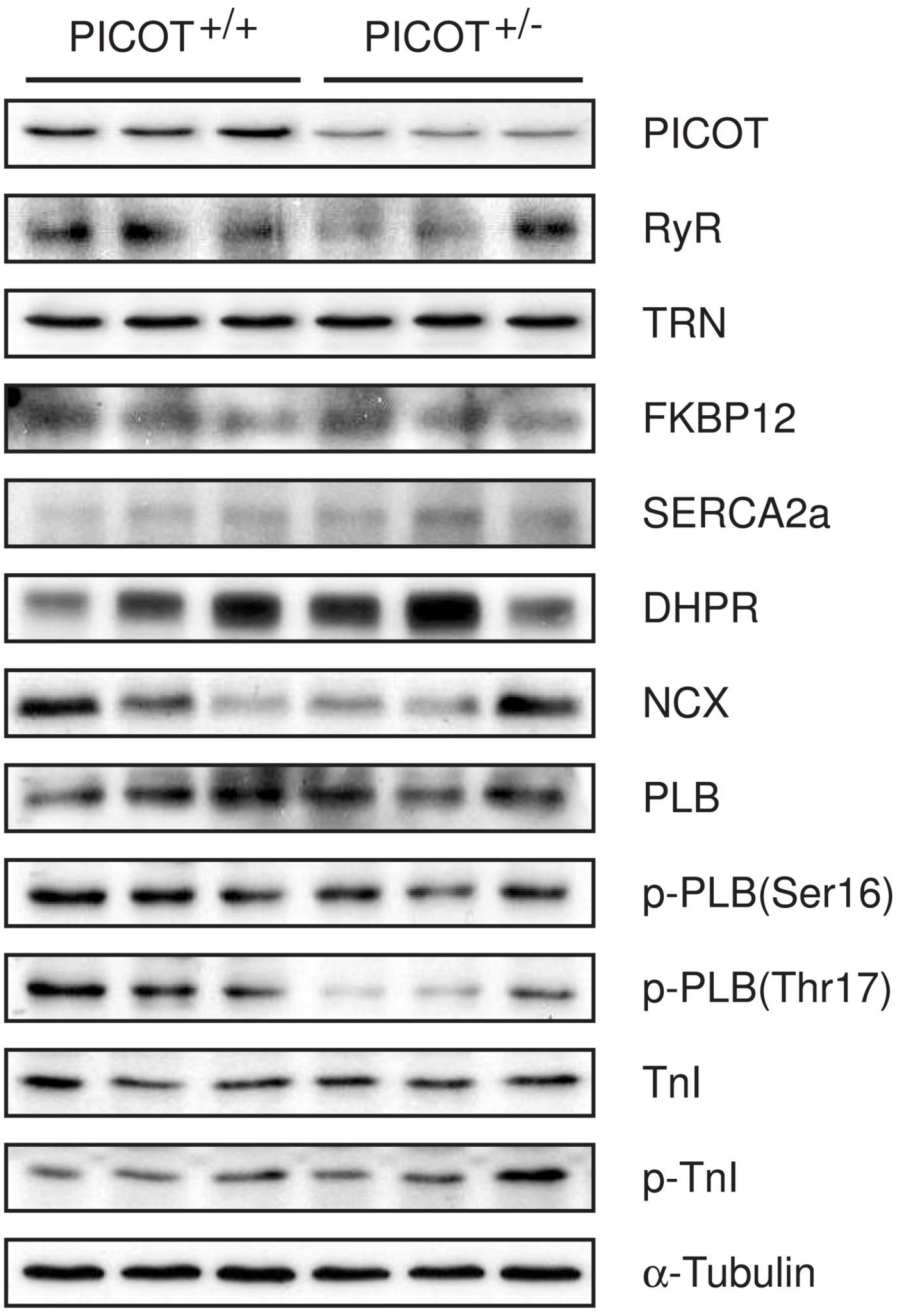


**Figure 5. Western blot analysis of heart lysates**

Heart lysates from *PICOT*$^{+/-}$ and *PICOT*$^{+/-}$ littermates were separated by SDS-PAGE, transferred to PVDF filter, and probed with antibodies against PICOT, PKC-interacting cousin of Thioredoxin; RyR, ryanodine receptor; TRN, triadin; FKBP12, FK506 binding protein 12; SERCA2a, sarcomeric reticular $Ca^{2+}$ ATPase 2a; DHPR, dihydropyridine receptor; NCX, $Na^{2+}$-$Ca^{2+}$ exchanger; PLB, phospholamban; p-PLB, phosphorylated PLB; TnI, troponin I; p-TnI, phosphorylated TnI. α-tubulin was used a loading control.